# Bioactive lipids as key regulators in atherosclerosis

Bot, M.

# 8 Hematopoietic Sphingosine 1-Phosphate Lyase Deficiency Decreases Atherosclerotic Lesion Development in LDL Receptor Deficient Mice

Martine Bot[1], Ilze Bot[1], Marijke M. Westra[1], Saskia C.A. de Jager[1], Peter J. Van Santbrink[1], Gerd Van der Hoeven[2], Marion J. Gijbels[3], Carsten Müller-Tidow[4], Gregor Varga[5], Theo J.C. Van Berkel[1], Paul P. Van Veldhoven[2], Jerzy-Roch Nofer[6,7], Erik A.L. Biessen[1,3]

[1]Division of Biopharmaceutics, Leiden/Amsterdam Center for Drug Research, Leiden University, Leiden, the Netherlands, [2]LIPIT, Department of Molecular Cell Biology, K.U. Leuven, Leuven, Belgium, [3]Experimental Vascular Pathology group, Department of Pathology, Maastricht University Medical Center, Maastricht, the Netherlands, [4]Department of Medicine, Hematology and Oncology, University Hospital Münster, Münster, Germany, [5]Institute of Experimental Dermatology, University of Münster, Münster, Germany, [6]Center for Laboratory Medicine, University Hospital Münster, Münster, Germany, [7]Leibniz-Institute for Arteriosclerosis Research, University of Münster, Münster, Germany.

*Submitted*

## Abstract

Sphingosine 1-phosphate (S1P), a bioactive lysosphingolipid, is a potent immunomodulator acting both intra- and extracellularly. It is implicated in various inflammatory diseases such as atherosclerosis. As intracellular S1P levels are tightly controlled by S1P lyase, we investigated the role of S1P lyase, encoded by *Sgpl1*, in hematopoietic cells on leukocyte homeostasis and atherosclerosis. High fat diet fed LDLr$^{-/-}$ chimeras with hematopoietic *Sgpl1*$^{-/-}$ showed a dramatic phenotype. First, S1P gradients were completely disrupted in hematopoietic *Sgpl1*$^{-/-}$ mice translating in reduced lymphocyte homing and mild lymphocytopenia in blood, lymph nodes and spleen and a concomitant enrichment of T-cell migration (CCR7, CXCR4, $S1P_1$) and activation (CD45RA, CD69) markers. Strikingly, splenocyte mitogenic and cytokine response to various stimuli (ConA, CCL19) was almost completely ablated in *Sgpl1*$^{-/-}$. Moreover, not only S1P-dependent leukocyte trafficking was quenched but also the response to other chemotactic factors including CCL19. Second, *Sgpl1*$^{-/-}$ chimeras displayed mild monocytosis, and altered cytokine patterns of macrophage secretome and plasma compatible with M1 polarization. Third, the hyperlipidemic response to western type diet was almost completely blunted in *Sgpl1*$^{-/-}$ chimeras due to impaired fat absorption, which may be linked to the aberrant microvilli architecture. These phenotypic changes were seen to culminate in reduced atherosclerotic plaque formation in *Sgpl1*$^{-/-}$ chimeras ($1.05*10^5$ μm$^2$ versus $1.62*10^5$ μm$^2$, P=0.02).
In conclusion, we here establish the critical importance of leukocyte S1P lyase in S1P-dependent lymphocyte surveillance, and in addition are the first to demonstrate a pivotal role as response modifier to chemotactic signals in general, of myeloid differentiation polarization, lipid homeostasis and atherogenesis, making it an attractive pharmaceutical target.

## Introduction

The biologically active lysosphingolipid sphingosine 1-phosphate (S1P) is an important lipid mediator generated from sphingosine upon cell activation and present in plasma and extracellular fluid at high nanomolar concentration[1,2]. Almost all cells of hematopoietic origin, such as platelets, mast cells, neutrophils, erythrocytes and mononuclear cells are able to store and release S1P, presumably via ATP binding cassette transporter C1[3-5].

A large body of evidence documents modulatory effects of S1P on lymphocyte proliferation, migration and cytokine secretion[6,7]. Moreover, S1P and its cognate receptor, $S1P_1$, are critically involved in maintaining proper lymphocyte egress from lymphoid organs[8-11]. In fact, S1P gradients between lymphoid organs (low [S1P]) on the one hand and circulation (high [S1P]) on the other hand are driving forces in lymphocyte fluxes from lymphoid organs to the periphery[7,12,13]. However, the actual regulation of S1P gradients remains elusive, as most cell types are able to generate S1P through ubiquitously expressed sphingosine kinases 1 and 2[14,15], and degrade it through S1P lyase or S1P phosphatases 1 and 2[1]. In addition to the effects on lymphocyte trafficking, S1P also plays a major role in endothelial integrity and confers protection against tumor necrosis factor (TNF)-α-induced monocyte-endothelial interactions[16,17]. Furthermore, S1P or its analogues are known to inhibit apoptosis in monocytes and bone marrow-derived macrophages[18] and to polarize macrophages towards less inflammatory M2 phenotype[19].

The S1P-induced impairment of T cell and monocyte/macrophage trafficking and activation may at least in part account for the beneficial effects exerted by this lysosphingolipid in animal models of inflammatory diseases such as ulcerating colitis, viral myocarditis, endotoxin-induced lung injury, or autoimmune encephalomyelitis[20-23]. As lymphocyte and macrophage activation within the arterial wall constitutes an essential step in the initiation and progression of atherosclerotic lesions[24], the potential involvement of S1P in the development of atherosclerosis has also been postulated. Actually, recent studies by us and others have shown that FTY720, which in its phosphorylated form (FTY720-P) is a synthetic S1P mimetic, reduced atherogenesis in mouse models of atherosclerosis, by causing sequestration of lymphocytes in lymph nodes and lymphocytopenia, impairing monocyte penetration into the arterial wall, and acting anti-inflammatory on macrophages and endothelium[19,25]. However, these studies left unanswered whether anti-atherogenic effects of FTY720 were completely attributable to S1P receptor signaling. Therefore, we sought to investigate the potential effects of increased endogenous S1P contents and signaling on atherosclerosis in hematopoietic S1P lyase (*Sgpl1*$^{-/-}$) deficiency. Here, we not only establish that hematopoietic S1P lyase deficiency increases S1P content in plasma and lymphatic organs, but are the first to show that, in parallel, it attenuates the development of atherosclerosis not only by modulating T lymphocyte and macrophage trafficking and function, but also by ameliorating diet-induced hyperlipidemia.

## Materials and Methods

*Animals*

All animal work was approved by the regulatory authorities of Leiden or Leuven and performed in compliance with the Dutch and Belgian government guidelines. LDL receptor deficient mice (LDLr$^{-/-}$, Jackson Laboratories) were bred in the local animal breeding facility. S1P lyase deficient (*Sgpl1*$^{-/-}$) and wild type littermates were obtained by crossing *Sgpl1*$^{+/-}$ mice, inbred in a C57Bl/6 background[26], in the animal housing facilities of the University of Leuven. The *Sgpl1*$^{+/-}$ non-inbred mouse was generated from gene-trapped ES cells (OST 58278) by Lexicon Inc. (Texas) on a fee basis.

*Irradiation and bone marrow transplantation*

One week before bone marrow transplantation female LDLr$^{-/-}$ recipients (12-13 and 13-19 weeks of age) (n=24 for atherosclerotic lesion analysis, n=12 for lipid homeostasis analysis and n=20 for migration studies) were given *ad libitum* drinking water supplemented with antibiotics (83 mg/L ciprofloxacin and 67 mg/L Polymixin B sulphate) and 6.5 g/L sugar. To induce bone marrow aplasia, female LDLr$^{-/-}$ mice were exposed to a single dose of 9 Gy (0.19 Gy/min, 200 kV, 4 mA) total body irradiation, using an Andrex Smart 225 Röntgen source (YXLON International, Copenhagen, Denmark) with a 6-mm aluminum filter, one day before transplantation. Bone marrow cell suspensions were isolated from 2-week old *Sgpl1*$^{-/-}$ and $^{+/+}$ littermates by flushing the femurs, tibias, humeri, radii and ulnas with phosphate buffered saline (PBS, 150 mmol/L NaCl, 1.5 mmol/L $NaH_2PO_4$, 8.6 mmol/L $Na_2HPO_4$, pH 7.4). Single-cell suspensions were prepared by passing the cells through a 70 µm cell strainer (BD, Breda, The Netherlands) and $5x10^6$ cells were injected into the tail vein of the irradiated recipients. The mice that underwent bone marrow transplantation were housed in sterile filter-top cages and were fed a sterile regular chow diet (RM3; Special Diet Services, Witham, United Kingdom) during 6 weeks and a Western type diet containing 0.25% cholesterol and 15% cocoa butter during 4 weeks (Western diet; Special Diet Services). During the experiment the weight of the animals was monitored and blood was collected via the tail vein once a week for lipid analysis or white blood cell analysis either by flow cytometry (FACScalibur or FACSCanto, BD Biosciences) or by automated differential cell count analysis (Sysmex, Goffin Meyvis BV, Etten Leur, The Netherlands).

*Lipid and lipoprotein analysis*

Total plasma cholesterol, triglycerides (Roche Diagnostics, Mannheim, Germany) and phospholipid (Spinreact, Sant Esteve de Bas, Spain) levels were quantified colorometrically by enzymatic procedures using Precipath (Roche) as internal standard. Plasma lipoprotein profiles were assessed by gel exclusion chromatography using a Superose 6 column equipped Smart™ micro FPLC system (Pharmacia, Uppsala, Sweden). For the analysis of sphingosine[27] and S1P, acidic methanolic extracts of plasma or tissues were fortified with internal standards, $C_{17}$-sphingosine (Toronto Research Chemicals) and $C_{17}$-S1P, prepared from $C_{17}$-sphingosine with recombinant human Sphk1[28], diluted with water and applied to a hydrophobic SPE cartridge. Compounds eluted with methanol, were derivatized with 6-aminoquinolyl-N-hydroxysuccinimidyl carbamate and subjected to normal phase SPE to separate the derivatized

sphingoid bases and their phosphate esters. After two selective hydrolysis steps, samples were separated by reversed phase HPLC (Symmetry C18-column 4.6x150; 5 µm; 100Å; Waters) with an increasing gradient of buffered methanol/acetonitrile coupled to fluorimetric analysis[27].

*Tissue harvesting*

Mice used for CCR7-dependent chemotaxis studies received an intraperitoneal injection of CCL19 (500 ng/mL; Peprotech, Rocky Hill, NJ) or phosphate buffered saline (PBS) as a control 24 hours before sacrifice. Mice were anesthetized by subcutaneous injection of ketamine (60 mg/kg, Eurovet Animal Health, Bladel, The Netherlands), fentanyl citrate and fluanisone (1.26 mg/kg and 2 mg/kg respectively, VetaPharma Ltd, Leeds, UK). After anesthesia mice were bled via orbital exsanguination, peritoneal leukocytes were isolated by flushing the peritoneal cavity with ice-cold PBS, and the thymus and lymph nodes (skin, heart and mesenteric) were dissected. Thereafter, the mice were perfused through the left cardiac ventricle with PBS. Subsequently, organs were excised, weighed (spleen, thymus and liver) and stored either on ice for use in flow cytometry analysis, in 4% Zinc Formalfixx (Shandon Inc, Thermo Fisher Scientific BV, Breda, The Netherlands) for histological analysis, or snap-frozen in liquid nitrogen for optimal RNA, DNA and lipid preservation. The latter specimens were stored at -80°C until further use. Single-cell suspensions were prepared of part of the spleen, mesenteric lymph nodes and thymus by passing crude cell suspensions through a cell strainer. Erythrocytes in blood and spleen suspensions were lysed by incubating the suspensions in erythrocyte lysis buffer (0.01 M Tris, 0.83% $NH_4Cl$, pH7.2) for 5 minutes on ice.

*Differential blood cell analysis*

Differential blood cell analysis was performed by automated differential cell count analysis (Sysmex, Goffin Meyvis BV, Etten Leur, The Netherlands) or by flow cytometry (FACSCalibur, FACSCANTO II or LSRII, BD) on whole blood, white blood cells, peritoneal leukocytes, and single-cell suspensions of spleen, lymph nodes, thymus and bone marrow. Monoclonal antibodies for flow cytometry were from BD, Breda, The Netherlands (CD4, CXCR4, CD8, CCR5 and streptavidin-PE), eBioscience, Zoersel-Halle, Belgium (CCR7, CD8, CD19, CD11b, GR1, CD71, CD11c, F4/80, MHCII and CD86), Abcam, Cambridge, UK ($S1P_1$, goat-anti-rabbit-FITC and donkey-anti-rabbit-PE) and US Biological/Immunosource, Zoersel-Halle, Belgium (CXCR3). For each FACS staining $2*10^5$ cells were incubated with antibody dilutions (0.25 µg for each antibody) in PBS plus 1% mouse serum at 4ºC.

*Plasma cytokine determination*

Mouse plasma cytokines (i.e. interleukin [IL]-6, IL-10, monocyte chemoattractant protein [MCP]-1, interferon [IFN]-γ, TNF-α and IL-12p70) were determined by a cytometric bead array (CBA, BD) on a FACSCalibur (BD). Calibration curves were established from standard solutions provided by BD. Aliquots of 50 µL undiluted mouse sera were used to determine the cytokine patterns. Analysis of calibration curves and samples was done using BD™ CBA software.

*Splenocyte proliferation and cytokine production*

Freshly isolated splenocytes were washed twice, resuspended in RPMI1640 (PAA Laboratories, Cölbe, Germany) containing 10% fetal calf serum (FCS, v/v), 2 mmol/L L-glutamine, 100 U/mL penicillin, 100 µg/mL streptomycin, and 50 µmol/L β-mercaptoethanol (RPMI complete), seeded at a density of $2*10^5$ cells/well in 96-well plates. Cells were incubated for 40 hours in RPMI complete or RPMI complete supplemented with S1P (100 nmol/L; Bio Connect BV, Huissen, The Netherlands) or concanavalin A (ConA; 2 µg/mL; Sigma, Zwijndrecht, The Netherlands). After 24 hours [$^3$H]thymidin (5.0 µCi/well; GE Healthcare, Eindhoven, The Netherlands) was added and cells were incubated for a further 16 hours. Thereafter, cells were centrifuged (5 min, 5000 rpm), washed 3 times with PBS, lysed with 0.1 mol/L NaOH, and cell-associated radioactivity was determined by scintillation spectrometry. Inflammatory cytokine levels (IL-2, IL-4, IL-10, IL-12 and INF-γ) in the supernatant were determined by commercially available ELISAs according to the instructions of manufacturer (eBioscience).

Assessment of T-cell proliferation by flow cytometry was done as described previously[29]. Briefly, $1*10^7$ splenocytes were incubated for 5 min at 37°C in PBS containing 0.5 µmol/L carboxyfluorescein diacetate succinimidyl ester (CFSE, Molecular Probes, Leiden, Netherland) in the dark after which cells were washed with PBS containing 1% FCS. CFSE-labelled splenocytes were plated in triplicates in 96-well plates ($1*10^5$ cells/well) and either kept in normal medium or stimulated with ConA (2 µg/mL) for 5 days. Cells were harvested, stained for CD4 and subsequently analyzed for proliferation by flow cytometry. Consecutive CFSE intensity peaks on flow cytometry were used as a measure of splenocyte proliferation.

*Functional characterization of peritoneal and bone marrow-derived macrophages*

Peritoneal macrophages (p-mφ) were harvested as described above. Bone marrow-derived macrophages (BM-mφ) were cultured from bone marrow isolated from chimeras in RPMI1640 supplemented with 20% FCS (v/v), 2 mmol/L L-glutamine, 100 U/mL penicillin, 100 µg/mL streptomycin, 1% non essential amino acids (v/v), 1% pyruvate (v/v), and macrophage colony-stimulating factor (M-CSF) for a week. After detachment of macrophages with 4 mmol/L EDTA, cells were resuspended in DMEM (PAA Laboratories) containing 10% FCS (v/v), 2 mmol/L L-glutamine, 100 U/mL penicillin, and 100 µg/mL streptomycin, and seeded in a 24-well plate at a density of $0.5*10^6$ cells/mL. After 16 hours non-adherent cells were removed and adherent macrophages were incubated for 24 hours in the absence or presence of lipopolysaccharide (LPS; 50 ng/mL; Salmonella Minnesota R595 (Re); List Biological Laboratories Inc. Campbell, CA) or IL-4 (100 ng/mL for p-mφ and 10 ng/mL for BM-mφ, Peprotech). IL-6, IL-10, IL-12, MCP-1 and TNF-α contents in medium were determined by commercially available ELISAs according to the instructions of manufacturer (eBioscience and BD). Total RNA was extracted as described previously[30]. RNA was reverse transcribed by M-MuLV reverse transcriptase (RevertAid, MBI Fermentas, St. Leon-Rot, Germany) and used for quantitative analysis of gene expression on ABI7500 Fast Real-Time PCR system (Applied Biosystems, Foster City, CA) as described previously[31], with murine hypoxanthine phosphoribosyltransferase (HPRT) as housekeeping gene (Table 1).

| Gene | Source | forward primer (5'-3') | reverse primer (5'-3') |
|---|---|---|---|
| Arginase 1 | NM_007482 | GGTTCTGGGAGGCCTATCTTACA | TCTTCACCTCCTCTGCTGTCTTC |
| CCL3 | NM_011337 | GCCACATCGAGGGACTCTTCA | GATGGGGGTTGAGGAACGTG |
| CCR2 | NM_009915 | AACTGTGTGATTGACAAGCACTTAGAC | TGACAGGATTAATGCAGCAGTGT |
| CCR5 | NM_009917 | GACTGTCAGCAGGAAGTGAGCAT | CTTGACGCCAGCTGAGCAA |
| IL-1α | NM_010554 | GCGCTCAAGGAGAAGACCAG | TGATACTTTTCCAGAAGAAAATGAGG |
| IL-1RA | NM_031167 | TTCATAGTGTGTTCTTGGGCATC | CGCTTGTCTTCTTCTTTGTTCTTG |
| IL-6 | M20572 | GAAGAATTTCTAAAAGTCACTTTGAGATCTAC | CACAGTGAGGAATGTCCACAAAC |
| IL-10 | NM_010548 | TCCCCTGTGAAAATAAGAGCA | ATGCAGTTGATGAAGATGTCAAA |
| IL-12 p35 | NM_008351 | AGTGAAAATGAAGCTCTGCATCC | GATAGCCCATCACCCTGTTGA |
| IL-12 p40 | NM_008352 | GATTCAGACTCCAGGGGACA | GGAGACACCAGCAAAACGAT |
| iNOS | NM_010927 | CCTGGTACGGGCATTGCT | GCTCATGCGGCCTCCTTT |
| MCP-1 | M19681 | GCATCTGCCCTAAGGTCTTCA | TTCACTGTCACACTGGTCACTCCTA |
| TNF-α | X02611 | GCCAGCCGATGGGTTGTA | AGGTTGACTTTCTCCTGGTATGAGA |
| HPRT | NM_013556 | TTGCTCGAGATGTCATGAAGGA | AGCAGGTCAGCAAAGAACTTATAG |

**Table 1.** RT-PCR primer sequences and sources for gene expression analysis of p-mφ and BM-mφ.

*Functional characterization of bone marrow*

For the functional characterization of bone marrow, cells were flushed from tibias and femurs with PBS and filtered through a cell strainer. Anucleated red blood cells were lysed with lysis buffer (0.15 mol/L $NH_4Cl$, 1 mmol/L $KHCO_3$, 0.1 mmol/L $Na_2$-EDTA, pH 7.3), and the remaining white blood cells were washed once with PBS. Cells were incubated with the appropriate antibodies in PBS containing 5% calf serum for 30 min on ice in a total volume of 50 µL. One ml PBS was added and the suspension was underlayered with 0.5 mL calf serum and centrifuged for 5 min at 1000 rpm, and the supernatant was discarded. All flow cytometry determinations were performed on FACSCalibur (BD) and data were analyzed by CellQuest software. Anti-murine B220 was from Caltag (San Francisco, CA), all other antibodies (murine CD34, CD41, Ter119, Gr1, CD14, Sca1, CD117) were purchased from BD Pharmingen. For colony assays with primary mouse bone marrow, $10^4$ cells per ml methylcellulose (Stem cell technologies, M3434) were seeded in 3 cm dishes and cultivated for 8-11 days. Colonies were counted and grouped according to their morphology.

*In vivo splenocyte homing*

Homing/migration of lymphocytes from *Sgpl1*$^{-/-}$ chimeras versus littermate controls towards spleens and lymph nodes were assessed as follows. Single cell suspensions of spleen lymphocytes from *Sgpl1*$^{-/-}$ chimeras (labeled for 30 min with 20 µmol/L orange-fluorescent tetramethylrhodamine [CMTMR], Invitrogen) and wild type controls (labeled for 15 min with 2 µmol/L CFSE, Invitrogen) were intravenously injected in the tail vein at a 1:1 ratio ($4*10^6$ labeled splenocytes in total)[32].

After 48 hours blood was collected via orbital exsanguination and mice were perfused through the left cardiac ventricle with PBS. Part of the spleen, and mesenteric lymph nodes were isolated and analyzed for presence of CFSE and CMTMR labeled spleen lymphocytes by flow cytometry. Subsequently, the mice were perfused with 4% Zinc Formalfixx and skin lymph nodes and the remainder of the spleen were

removed and stored in 4% Zinc Formalfixx for histological analysis.

*Histological and morphometric analysis*
For analysis of spontaneous atherosclerosis, the aortic root was embedded in Tissue-Tek and transverse 10 µm cryosections throughout the aortic valve area were prepared and mounted in order on series of slides. Sections were stained with Oil Red O and hematoxylin (Sigma). Cross-sections with maximal stenosis were used for morphometric analysis on a DM-RE microscope with Leica Qwin image analysis software (Leica Microsystems B.V., Rijswijk, the Netherlands), as described previously[33]. Corresponding sections were stained with antibodies directed against mouse macrophages (monoclonal mouse $IgG_{2a}$, clone MOMA-2, dilution 1:50; Sigma Diagnostics, St. Louis, MO) and lymphocytes (CD3 clone SP7, Immunologic, Duiven, The Netherlands). Sections were stained for collagen using Masson's trichrome (Sigma). Cryosections of 5 µm were prepared from liver, spleen, thymus and lymph nodes. Sections were stained with hematoxylin and eosin (Merck Diagnostica, Darmstadt, Germany), Oil Red O (Sigma) and hematoxylin (liver and spleen) and for CD3 (spleen, lymph nodes and thymus). Paraffin sections of 4 µm were prepared from the intestine which were stained with periodic acid-Schiff (PAS).

*Lipid and gene expression analysis of liver and intestine*
Lipids were extracted from liver tissue by a Bligh and Dyer extraction[34]. Extracted lipids were dissolved in 1% Triton by sonication. Protein contents were analyzed by BCA assay (Pierce Biotechnology, Thermo Fisher Scientific BV). Total cholesterol, triglyceride and phospholipid contents of liver extracts were quantified as described above. For all mice part of a liver lobule and a segment of the intestine were used for total RNA extraction as described previously[30]. Quantitative analysis of gene expression was performed as described above (Table 2).

*Lipid homeostasis studies*
[$^3$H]cholesterol (0.1 mCi) was resuspended in 4 mL of an ethanol:olive oil mixture (1:9 v:v) and 200 µL of this mixture was administered by oral gavage to *Sgpl1*$^{-/-}$ chimeras and wild type controls (n=6 per group). At 0, 1, 2, 3, and 4 hours, blood samples were collected via tail vein puncture and plasma uptake of [$^3$H]cholesterol was determined by scintillation spectrometry. Very low-density lipoprotein (VLDL) production was analyzed after intravenous injection of mice with Triton WR1339/ Tyloxapol (500 mg/kg bodyweight, Sigma) in 0.9% NaCl. At 0, 1, 2, 3, and 4 hours, blood samples were collected via tail vein puncture and accumulation of triglyceride in plasma was measured as described above. Plasma lipoprotein lipase (LPL) activity was determined in blood samples drawn before and after an intravenous bolus injection of heparin (0.1 U/g bodyweight; Leo Pharma BV, Breda, The Netherlands). The lipolytic activity of pre- and post-heparin plasma was measured after addition of a radiolabeled triolein emulsion as described by Zechner *et al.*[35,36].

*Genotyping*
Genomic DNA from bone marrow was isolated using DNA extraction columns (Qiagen, Venlo, the Netherlands) and used for validation of bone marrow repopulation after transplantation. Primer sets for wild type S1P lyase allel (forward 5'- TGATAGGGCT-

GAAAACCACTG and reverse 5'- TCAGAAGCAAAACTGCCTTG) and the mutated allele, containing a β-geo insertion, (forward 5'-CGAATACCTGTTCCGTCATAGC and reverse 5'-ACCACTACCATCATCAATCCGGTAG) were used.

| Gene | Source | forward primer (5'-3') | reverse primer (5'-3') |
|---|---|---|---|
| ABCA1 | NM_013454 | GGTTTGGAGATGGTTATACAATAGTTGT | TTCCCGGAAACGCAAGTC |
| ABCB4 | NM_008830 | AGGCAGCGAGAAACGGAAC | TGGTTGCTGATGCTGCCTAG |
| ABCB11 | NM_021022 | TGGAAAGGAATGGTGATGGG | CAGAAGGCCAGTGCATAACAGA |
| ABCG1 | NM_009593 | AGGTCTCAGCCTTCTAAAGTTCCTC | TCTCTCGAAGTGAATGAAATTTATCG |
| ABCG5 | NM_031884 | TGGCCCTGCTCAGCATCT | ATTTTTAAAGGAATGGGCATCTCTT |
| ABCG8 | NM_026180 | CCGTCGTCAGATTTCCAATGA | GGCTTCCGACCCATGAATG |
| Acat2 | NM_009338 | CAGAGGGCCAAGGTGGC | CAACCTGCCGTCAAGACATG |
| Apoc1 | BC019398 | CGGGCAGCCATTGAACATA | TTGCCAAATGCCTCTGAGAAC |
| Apoc2 | NM_009695 | AAGATGACTCGGGCAGCCT | CAGAGGTCCAGTAACTTAAGAGGGA |
| Apoc3 | NM_023114 | GTACAGGGCTACATGGAACAAGC | CGGACTCCTGCACGCTACTT |
| α-actin | X03672 | AACCGTGAAAAGATGACCCAGAT | CACAGCCTGGATGGCTACGTA |
| CD3 | NM_007648.4 | ACTATGAGCCCATCCGCAAA | GAAGGCGATGTCTCTCCTATCTG |
| CD68 | NM_009853 | CCTCCACCCTCGCCTAGTC | TTGGGTATAGGATTCGGATTTGA |
| Cyp3a11 | NM_007818 | GGATGAGATCGATGAGGCTCTG | CCAGGTATTCCATCTCCATCACA |
| Cyp7a1 | NM_007824 | CTGTCATACCACAAAGTCTTATGTCA | ATGCTTCTGTGTCCAAATGCC |
| Cyp27 | AK004977 | GTGTCCCGGGATCCCAGTGT | CTTCCTCAGCCATCGGTGA |
| GAPDH | NM_008084 | TCCATGACAACTTTGGCATTG | TCACGCCACAGCTTTCCA |
| HMG-CoAR | M62766 | TCTGGCAGTCAGTGGGAACTATT | CCTCGTCCTTCGATCCAATTT |
| HPRT | NM_013556 | TTGCTCGAGATGTCATGAAGGA | AGCAGGTCAGCAAAGAACTTATAG |
| LPL | NM_008509 | CCAGCAACATTATCCAGTGCTAG | CAGTTGATGAATCTGGCCACA |
| Lrp1 | NM_008512 | TGGGTCTCCCGAAATCTGTT | ACCACCGCATTCTTGAAGGA |
| MARCO | MMU18424 | AAAGGGTCAAAAAGGCGAATCT | AACTTCAGCTCGGCCTCTGTT |
| MTP | L47970 | AGCTTTGTCACCGCTGTGC | TCCTGCTATGGTTTGTTGGAAGT |
| Npc1l1 | NM_207242 | CTACACGGCCTGGTCTTCCT | AAGGGGTACTGTGGGCAAG |
| Scd1 | NM_009127 | TACTACAAGCCCGGCCTCC | CAGCAGTACCAGGGCACCA |
| SHP | L76567 | CTATTCTGTATGCACTTCTGAGCCC | GGCAGTGGCTGTGAGATGC |
| SRBI | NM_016741 | GGCTGCTGTTTGCTGCG | GCTGCTTGATGAGGGAGGG |
| SREBP-1 | AB017337 | GACCTGGTGGTGGGCACTGA | AAGCGGATGTAGTCGATGGC |
| 36B4 | NM_007475 | GGACCCGAGAAGACCTCCTT | GCACATCACTCAGAATTTCAATGG |

**Table 2.** RT-PCR primer sequences and sources for gene expression analysis of liver and intestine.

*Statistical analysis*

Values are expressed as mean ± SEM. A 2-tailed Student's t-test was used to compare individual groups of animals. To determine significance of the relative mRNA expression levels, statistical analysis was performed on ΔCt values. Curve-fit analysis was performed for uptake of [$^3$H]cholesterol and for VLDL production. A level of $P<0.05$ was considered significant.

## Results

*Assessment of chimerism and S1P levels in hematopoietic Sgpl1$^{-/-}$ chimeras*

DNA analysis of bone marrow from *Sgpl1*$^{-/-}$ transplanted animals showed >90% repopulation of *Sgpl1*$^{-/-}$ bone marrow (Figure 1A). *Sgpl1*$^{-/-}$ chimerism did not affect body weight. Hematopoietic *Sgpl1*$^{-/-}$ led to a profound increase in S1P content in spleen (90-fold, P<0.001) and lymph nodes (47-fold, P<0.01), while total S1P levels in thymus (2.2-fold, P<0.05) and plasma (1.25-fold, P<0.01) were only modestly elevated (Figure 1B).

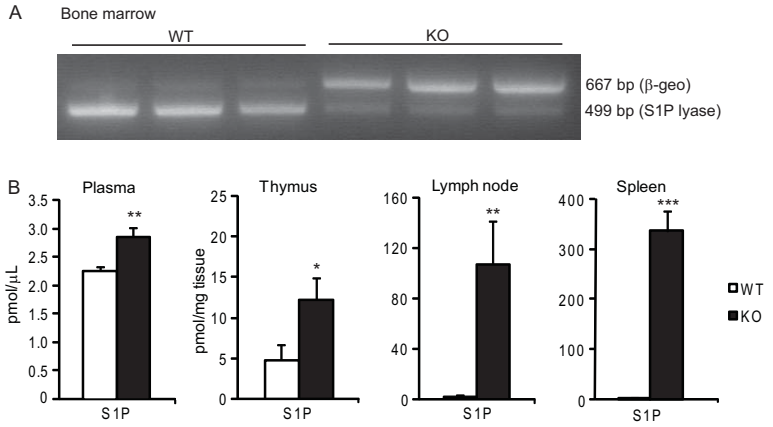


**Figure 1.** (A) Genotyping of the bone marrow showed >90% repopulation of the bone marrow for *Sgpl1*$^{-/-}$. (B) Effect of hematopoietic *Sgpl1*$^{-/-}$ on plasma S1P concentration and S1P content of thymus, lymph node, and spleen. *P< 0.05, **P< 0.01, ***P< 0.001.

*Hematopoietic Sgpl1*$^{-/-}$ *chimeras display reduced T lymphocyte numbers and altered T cell subpopulations*

A first indication of perturbed lymphoid organisation was provided by the significantly increased spleen weight of *Sgpl1*$^{-/-}$ chimeras (+48%, P<0.005, data not shown), whereas thymic weight showed a significant reduction (-38%, P<0.001, data not shown). Next, we monitored lymphocyte abundance in blood and lymphatic organs of transplanted mice. In keeping with earlier findings on pharmacological S1P lyase inhibition with 2-acetyl-4-tetrahydroxybutylimidazole (THI)[12], blood lymphocyte counts were decreased from 3.2 to 1.1*10$^6$ cells/mL (-66%, P<0.001) in mice with hematopoietic *Sgpl1* deficiency. Flow cytometry confirmed that *Sgpl1*$^{-/-}$ chimeras had sharply decreased CD4$^+$ T-cell levels in blood, lymph nodes, spleen (>-60%, P<0.001, Figure 2A) and peritoneum (-50%, P<0.001, data not shown). CD8$^+$ T cells showed a similar pattern of about 50-60% decrease in blood, lymph nodes and spleen (P<0.005, Figure 2B), but no changes were seen in the peritoneal leukocyte population (data not shown). Immunohistochemistry revealed decreased CD3$^+$ T cell content of spleen and aberrant germinal center morphology (Figure 2C). Surprisingly, and in contrast to effects of systemic S1P lyase inhibition by THI[12] and after S1P activation (FTY720), no accumulation of T cells was evident in lymph nodes. Thymic CD4$^+$ and CD8$^+$ T cell contents were only marginally decreased (-6% and -23%, respectively, P<0.05, data not shown).

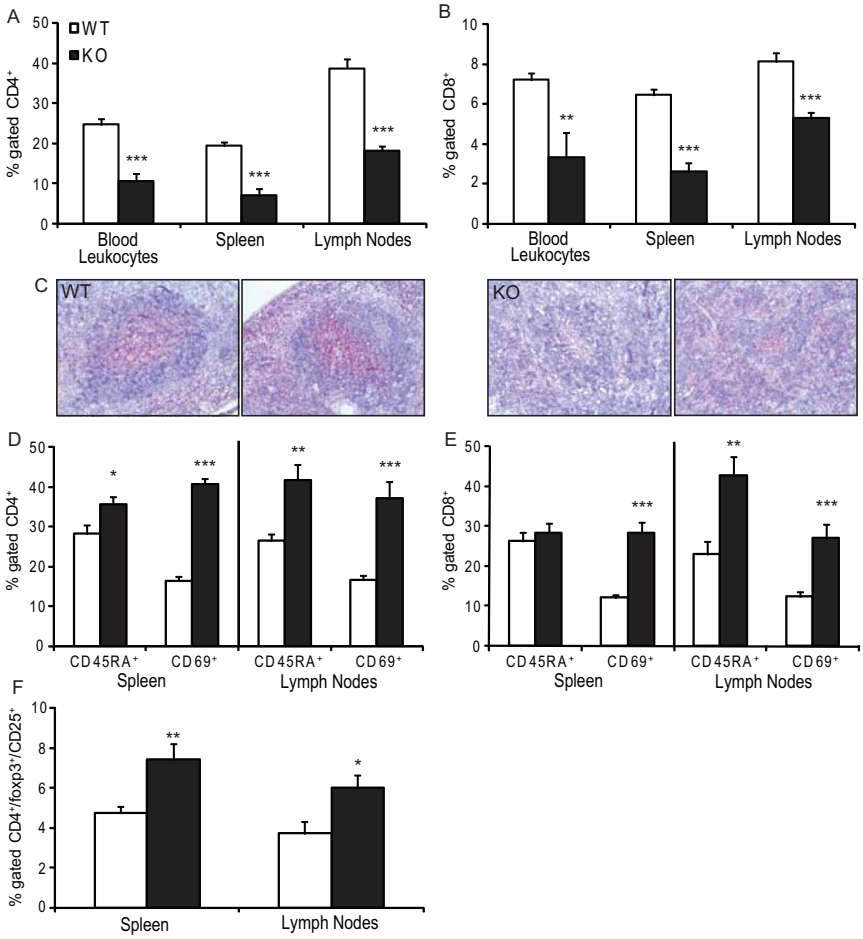


**Figure 2.** Effect of hematopoietic *Sgpl1*$^{-/-}$ on number and activation status of T cells. *Sgpl1*$^{-/-}$ chimeras show reduced number of circulating, spleen and lymph node CD4$^+$ (A) and CD8$^+$ (B) T cells. (C) CD3 staining shows absence of normal germinal centre morphology in spleens of *Sgpl1*$^{-/-}$ chimeras. (D) CD4$^+$ T cells are enriched in CD69$^+$ and CD45RA$^+$ cells in spleen and lymph nodes of *Sgpl1*$^{-/-}$ chimeras. (E) CD8$^+$ T cells are also enriched in CD69$^+$ and CD45RA$^+$ cells in spleen and lymph nodes of *Sgpl1*$^{-/-}$ chimeras. (F) *Sgpl1*$^{-/-}$ chimeras show a relative increase in regulatory T cells in the spleen and lymph nodes. *P< 0.05, **P< 0.01, ***P< 0.001.

The overall reduction in T cell numbers seen in *Sgpl1*$^{-/-}$ chimeras was paralleled by specific changes in CD4$^+$ and CD8$^+$ subsets. In lymph nodes, spleen and peritoneum CD4$^+$ and CD8$^+$ T cells were enriched in CD69, an early activation marker and a putative lymphatic retention signal (P<0.001, Figure 2D, 2E)[37,38]. A similar enrichment was seen for CD45RA, a marker of naïve T cells as well as of effector CD8$^+$ T cells (P<0.05, Figure 2D, 2E). Regulatory T cell (CD4$^+$/foxp3$^+$/CD25$^+$) numbers in spleen and lymph nodes were moderately increased in *Sgpl1*$^{-/-}$ chimeras (respectively 4.8% to 7.4% and 3.7% to 6.0%, P<0.02, Figure 2F). In contrast to T cells, hematopoietic S1P lyase deficiency did not noticeably influence total B cell (CD19) numbers in blood, lymph nodes and peritoneum, although we did observe a significant 47% decrease in B cell precursors (CD34$^-$/B220$^+$) in bone marrow (P<0.001, Figure 3A).

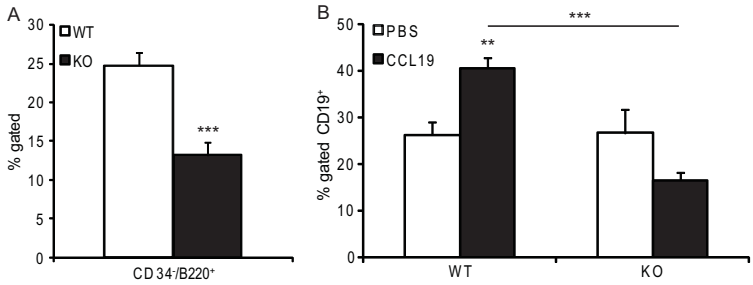


**Figure 3.** (A) Flow cytometry analysis of bone marrow B cell precursors ($CD34^{-}/B220^{+}$) showed a 47% decrease. (B) Upon intraperitoneal CCL19 injection wild type transplanted animals showed B cell accumulation of 54% in blood, which was not seen in the *Sgpl1*$^{-/-}$ chimeras. **P< 0.01, ***P< 0.001.

*Lymphocyte function is impaired in Sgpl1*$^{-/-}$ *chimeras*

In addition to changes in lymphocyte counts and subset pattern, hematopoietic absence of S1P lyase also affected lymphocyte function. Stimulation of splenocytes with ConA (2.0 µg/mL) led to a potent mitogenic response in cells from wild type but not *Sgpl1*$^{-/-}$ transplanted animals (Figure 4A, 4B). This differential proliferative capacity was even more pronounced in mice challenged by intraperitoneal CCL19 injection emulating a peripheral inflammatory response (Figure 4C). Splenocyte dysfunction in *Sgpl1*$^{-/-}$ chimeras was also illustrated by the failure of splenocytes from CCL19-treated mice to secrete IL-2 and IL-4 (Figure 4D, 4E). In addition, *Sgpl1*$^{-/-}$ chimeras showed decreased rather than increased (*Sgpl1*$^{+/+}$) plasma IL-12 and TNF-α levels in response to CCL19 challenge, reflecting a reduced inflammatory responsiveness in these animals (Figure 4F, 4G).

*Disturbed T lymphocyte trafficking in Sgpl1*$^{-/-}$ *chimeras*

Since T cell egress from secondary lymphoid tissue is primarily mediated by migration along S1P gradients, we next assessed T-cell trafficking in *Sgpl1*$^{-/-}$ chimeras. Flow cytometry analysis of lymphoid organs and blood at 48 hours after injection of a 1:1 mixture of CMTMR-labeled *Sgpl1*$^{-/-}$ versus CFSE-labeled wild type splenocytes into $LDLr^{-/-}$ showed a reduced presence of the former in spleen (-42%), lymph nodes (-25%) and the blood (-57%, P<0.05, Figure 5A). This was confirmed by fluorescence microscopic analysis of lymph node and spleen (Figure 5B, 5C).

Since $S1P_1$ receptor is thought to mediate S1P directed lymphocyte trafficking and S1P analogues were shown to quench $S1P_1$ expression[10,12], we next measured the T-cell $S1P_1$ expression by flow cytometry. Contrary to our expectations, the $S1P_1^+$ T cells were overrepresented within the $CD4^+$ and $CD8^+$ population in blood, peritoneal leukocytes, lymph nodes and spleen, while S1P mean fluorescence per cell did not change, suggesting sensitization to S1P signaling (Figure 6A, 6B, data not shown). Further assessment of $CD4^+/S1P_1^+$ T cells in the leukocyte population revealed that this cell subset was decreased in blood while increased in the lymph nodes (Figure 6C). As S1P signaling seems not to be perturbed in *Sgpl1*$^{-/-}$ we set out to address whether the T-cell response to other chemotactic signals was affected. $CD4^+$ and $CD8^+$ T cell populations in *Sgpl1*$^{-/-}$ bone marrow transplanted animals both displayed a striking enrichment in migration markers CCR7 and CXCR4 (Figure 6A, 6B).

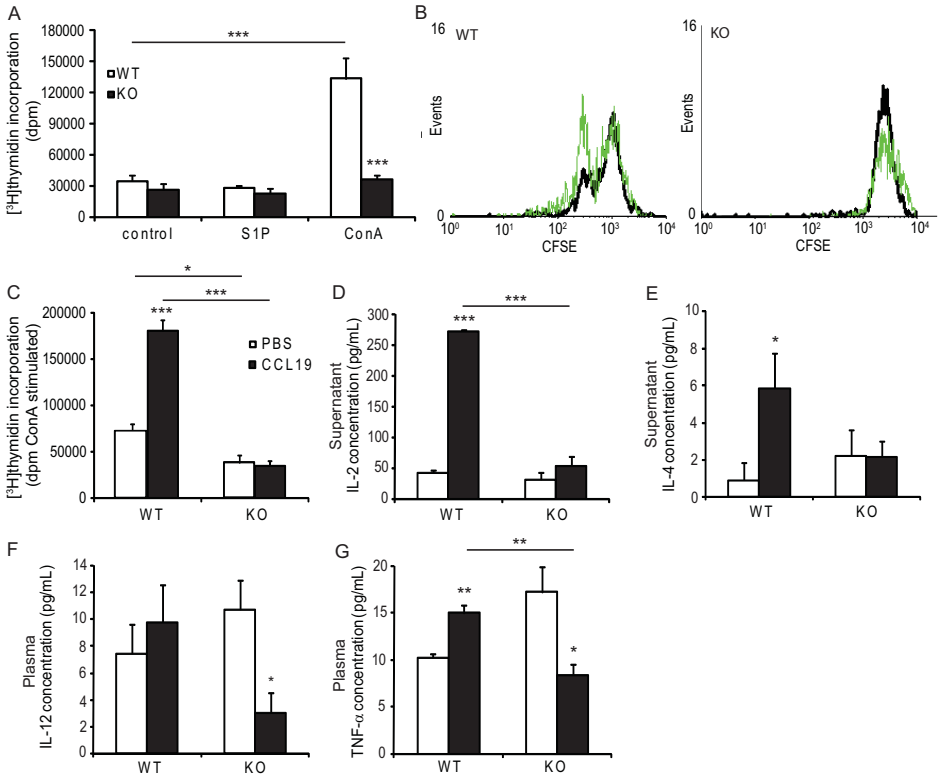


**Figure 4.** Effect of *Sgpl1*$^{-/-}$ chimerism on the mitotic and inflammatory response of splenocytes to S1P or ConA. (A,B) While splenocytes from *Sgpl1*$^{+/+}$ transplanted mice show a normal proliferative response, the mitotic response of splenocytes isolated from *Sgpl1*$^{-/-}$ chimeras to ConA (2 µg/mL) is completely abolished. (C) This abolishment of mitotic response is even more pronounced when splenocytes were isolated 24 hours after intraperitoneal CCL19 injection. Supernatant of these assays was used for cytokine analysis. (D,E) ConA-stimulated splenocytes of the CCL19-injected control animals show an induction in both IL-2 and IL-4 secretion, while this response is abolished in the *Sgpl1*$^{-/-}$ chimeras. (F,G) The CCL19-injected *Sgpl1*$^{-/-}$ chimeras show a reduction of plasma IL-12 and TNF-α, while in case of TNF-α the controls even show an increase indicating abolishment of the pro-inflammatory response. *P< 0.05, **P< 0.01, ***P< 0.001. dpm, disintegrations per minute.

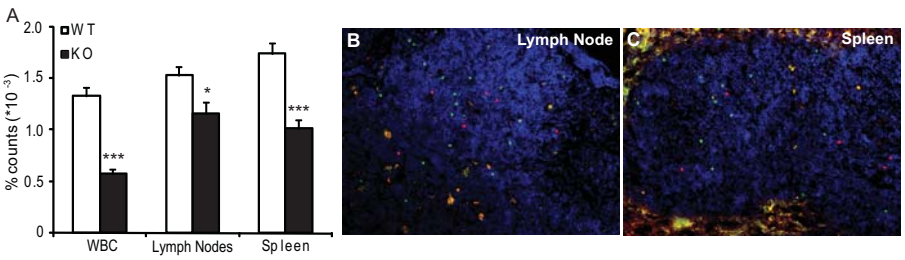


**Figure 5.** Splenocyte homing capacity is also disturbed in *Sgpl1*$^{-/-}$ chimeras. (A) Flow cytometry analysis of lymphoid organs and circulation at 48 hours after injection of a 1:1 mixture of CMTMR-labeled *Sgpl1*$^{-/-}$ versus CFSE-labeled wild type lymphocytes into LDLr$^{-/-}$ showed a reduced presence of the *Sgpl1*$^{-/-}$ lymphocytes in spleen, lymph nodes and the blood (WBC, white blood cells). This was confirmed by fluorescence microscopic analysis of lymph node (B) and spleen (C). *P< 0.05, ***P< 0.001.

The enrichment of the CCR7$^+$ subset within the T cell population in *Sgpl1*$^{-/-}$ transplanted animals prompted the question whether the migration response toward the cognate chemokines (e.g. CCL19) was altered in S1P lyase deficiency. Intraperitoneal injection of CCL19 in wild type transplanted animals increased the mobilization of both CD4$^+$ and CD8$^+$ T cells, and in particular the CCR7$^+$ and CXCR4$^+$ subsets, from blood by 30% (P<0.05, Figure 6D-F), while no apparent changes were seen in the lymph nodes or spleen (data not shown). Surprisingly, B cells were mobilized to blood in wild type transplanted animals (+54%, Figure 3B). By contrast, CCL19-elicited T-cell mobilization from blood and B-cell mobilization to blood did not occur in *Sgpl1*$^{-/-}$ chimeras (Figure 6D, 3B).

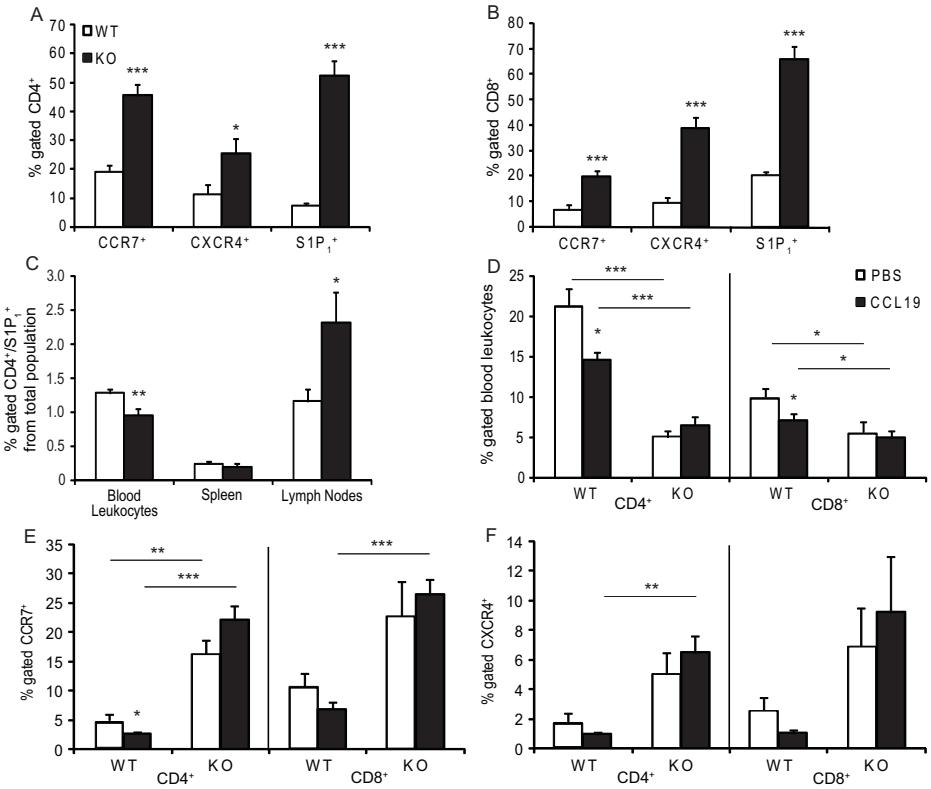


**Figure 6.** Effect of hematopoietic *Sgpl1*$^{-/-}$ on migration markers of T cells. (A,B) *Sgpl1*$^{-/-}$ chimeras show enrichment for CCR7, CXCR4 and $S1P_1$ in the CD4$^+$ and CD8$^+$ T-cell populations. (C) In the total leukocyte population, the relative number of CD4$^+$/S1P$^+$ T cells is mildly decreased in blood and 2-fold increased in lymph nodes, indicative for decreased egress in spite of $S1P_1$ receptor expression. (D) Intraperitoneal injection of CCL19 causes re-allocation of T-cell populations in the blood of the control animals, while these changes are absent in the *Sgpl1*$^{-/-}$ chimeras. (E,F) These re-allocations in the control animals concur with reductions in T cells expressing migration markers, while this is not seen in the *Sgpl1*$^{-/-}$ chimeras. *P< 0.05, **P< 0.01, ***P< 0.001.

*Increased monocyte and neutrophil numbers in Sgpl1*$^{-/-}$ *chimeras*

Both blood monocyte and neutrophil counts were markedly increased in *Sgpl1*$^{-/-}$ animals as assessed by differential cell count analysis (0.2 to 0.6*10$^6$ cells/mL and 0.5 to 1.8*10$^6$ cells/mL, respectively, P<0.005) and by flow cytometry (CD11b$^+$ monocytes:

+2.7-fold, P<0.001; CD11b$^{+}$/GR1$^{+}$/CD71$^{-}$ neutrophils: +2.2-fold, P<0.001) (Figure 7A). A similar increase in CD11b$^{+}$ cells was seen in the peritoneum (1.8-fold, P< 0.001, data not shown). CD11b$^{+}$/GR1$^{+}$ granulocyte precursors in bone marrow were elevated (+27%, P<0.001), while no effects were seen CD14$^{+}$/GR1$^{+}$ macrophage precursors (Figure 7B). This could be at least in part attributed to an increased GM-CSF and G-CSF dependent myelopoiesis of bone marrow cells in *Sgpl1*$^{-/-}$ chimeras (P<0.005, Figure 7C). Moreover, plasma MCP-1 levels, which drive stromal efflux of monocytes, were decreased in *Sgpl1*$^{-/-}$ chimeras, as was MCP-1 production at mRNA and protein level in bone marrow-derived macrophages from *Sgpl1*$^{-/-}$ chimeras (Figure 7D,7E). Surprisingly, gene expression analysis of bone marrow-derived macrophages revealed increased CCR2 expression in *Sgpl1*$^{-/-}$ chimeras (Figure 7F).

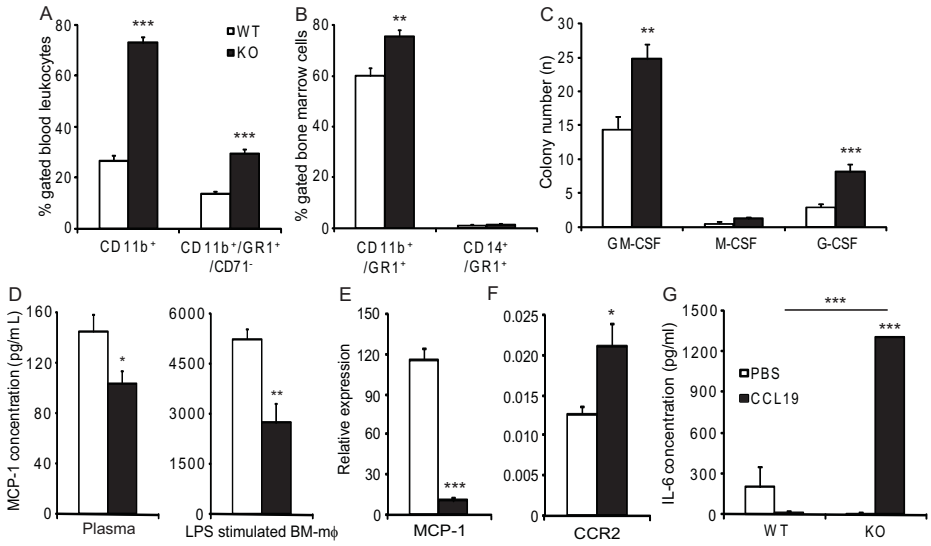


**Figure 7.** Effect of *Sgpl1*$^{-/-}$ chimerism on monocyte and neutrophil numbers. (A) *Sgpl1*$^{-/-}$ chimeras show increased numbers of CD11b$^{+}$ (monocytes) and neutrophils (CD11b$^{+}$/GR1$^{+}$/CD71$^{-}$) in the circulation. (B) In bone marrow the increase in neutrophils is already noticeable at the level of the precursors, while this is not the case for the monocytes. (C) Growth-stimulation of the bone marrow shows that GM-CSF and G-CSF both can induce increased colony formation of the bone marrow from the *Sgpl1*$^{-/-}$ chimeras, while no effect was seen upon stimulation with M-CSF, indicating an enhanced granulocyte response. (D) Analysis of plasma and bone marrow-derived macrophage (BM-mφ) supernatant shows a reduced MCP-1 generation in the *Sgpl1*$^{-/-}$ chimeras indicating a disruption in migratory response. This disruption is further demonstrated by decreased expression of MCP-1 (E) and increased CCR2 expression (F) in bone marrow-derived macrophages. (G) Peritoneal macrophages of *Sgpl1*$^{-/-}$ chimeras show an induced inflammatory IL-6 response after intraperitoneal CCL19 injection. *P< 0.05, **P< 0.01, ***P< 0.001.

As S1P$_1$ agonists were previously shown to act anti-inflammatory on macrophages[19,39], we next investigated the inflammatory status of *Sgpl1*$^{-/-}$ macrophages. To our surprise, peritoneal macrophages from CCL19-challenged *Sgpl1*$^{-/-}$ chimeras demonstrated an increased IL-6 response, which was not seen in cells from wild type controls indicating a pro-inflammatory phenotype (P<0.001, Figure 7G). Expression analysis on *Sgpl1*$^{-/-}$ versus $^{+/+}$ BM-derived macrophages confirmed this pro-inflammatory phenotype as shown by increased expression of pro-inflammatory cytokines IL-6, TNF-α and IL-1α and the classical activation (M1) cytokine IL-12 (P<0.001, Fig-

ure 8A-D). Conversely, expression of inducible nitric oxide synthase (iNOS), which is also an M1-type macrophage marker, was significantly reduced (P<0.001, Figure 8E).

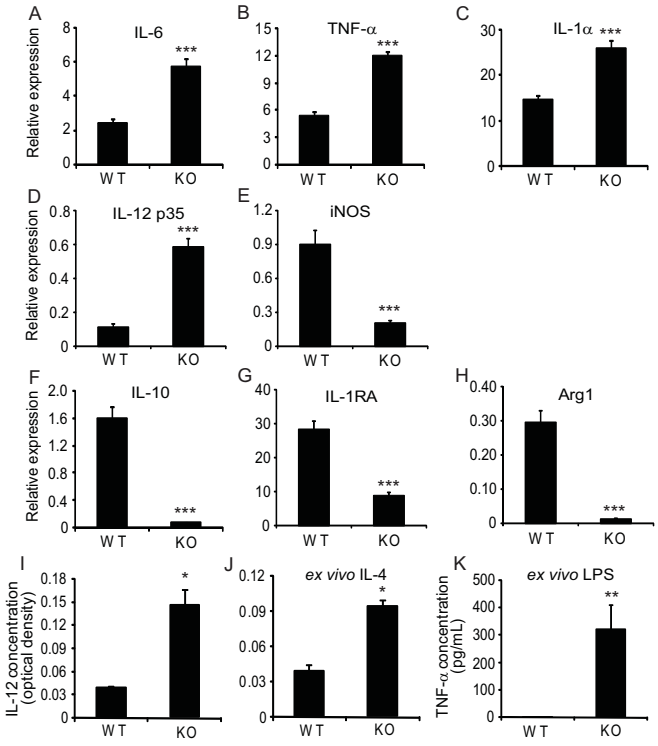


**Figure 8.** Phenotypic analysis of *Sgpl1*$^{-/-}$ chimera macrophages. Gene expression analysis of LPS-stimulated BM-mφ indicate a pro-inflammatory phenotype of *Sgpl1*$^{-/-}$ macrophages as shown by increased expression of IL-6 (A), TNF-α (B), IL-1α (C) and the M1 phenotype marker IL-12 (D), while iNOS expression, which is also an M1-phenotype marker, is decreased (E). Expression of typical M2 markers, such as IL-10 (F), IL-1RA (F) and arginase 1 (Arg1) (H), was decreased again indicative for a pro-inflammatory phenotype. Furthermore, after intraperitoneal CCL19 injection p-mφ of *Sgpl1*$^{-/-}$ chimeras show an induced inflammatory IL-12 response both in normal medium (I) and upon *ex vivo* IL-4 stimulation (J). In addition, BM-mφ show an increased LPS-induced TNF-α secretion (K). *P< 0.05, **P< 0.01, ***P< 0.001.

In contrast to M1-phenotype markers, alternative activation (M2) markers, such as IL-10, IL-1 receptor antagonist (IL-1RA) and arginase 1, were downregulated in *Sgpl1*$^{-/-}$ animals (Figure 8F-H). Additional evidence for the pro-inflammatory phenotype of *Sgpl1*$^{-/-}$ macrophages was provided by augmented IL-12 secretion of unstimulated and IL-4-stimulated *Sgpl1*$^{-/-}$ peritoneal macrophages and by increased LPS-induced TNF-α secretion of *Sgpl1*$^{-/-}$ BM-derived macrophages (Figure 8I-K).

*Hematopoietic Sgpl1*$^{-/-}$ *ameliorates lipid homeostasis*

Plasma total cholesterol, triglycerides and phospholipids in *Sgpl1*$^{-/-}$ and *Sgpl1*$^{+/+}$ transplanted mice did not differ when mice were fed a standard chow diet. However, on Western type diet the *Sgpl1*$^{-/-}$ transplanted mice displayed significantly lower total cholesterol, triglycerides and phospholipid levels (P<0.02, Figure 9A-C) and gener-

ally a less pro-atherogenic plasma lipoprotein profile (P<0.05, Figure 9D-F). Transfer of intestinal cholesterol to plasma was significantly decreased in *Sgpl1*$^{-/-}$ chimeras as judged from the delayed uptake of orally administered [$^3$H]cholesterol (P<0.05, Figure 9G).

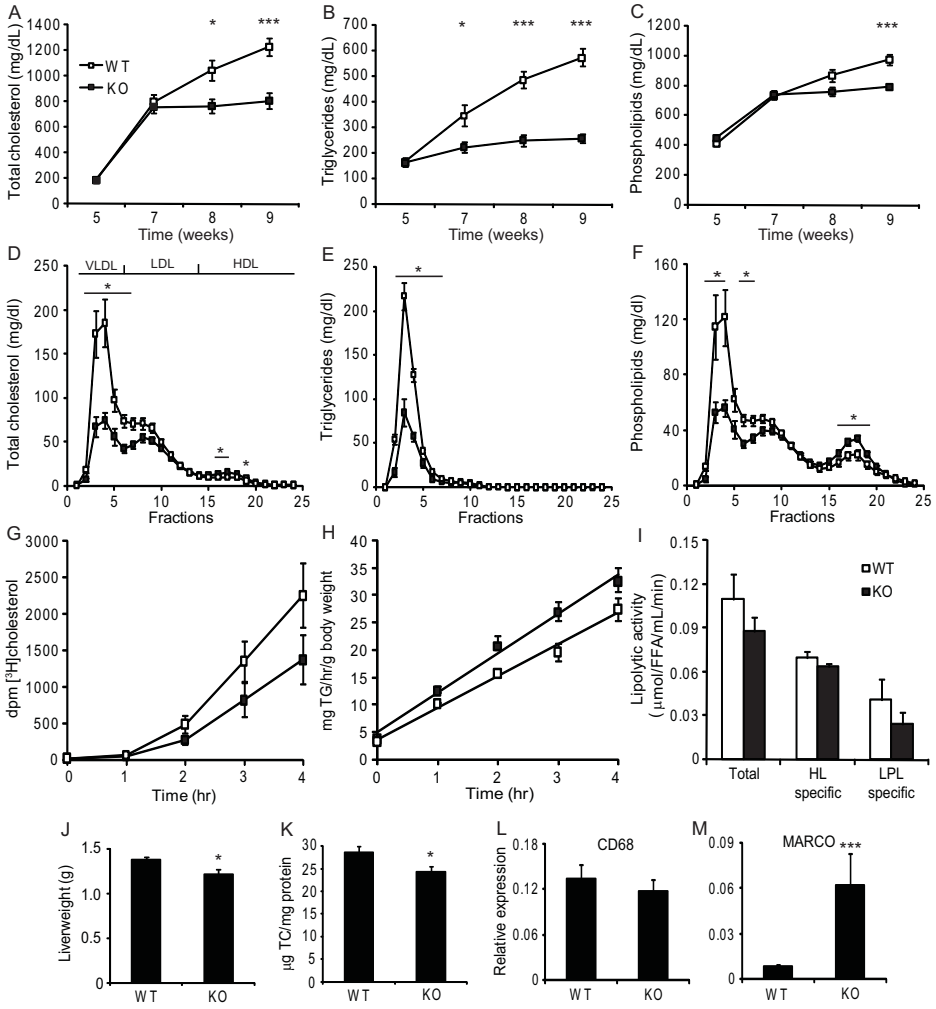


**Figure 9.** Effects of *Sgpl1*$^{-/-}$ chimerism on lipid profile and metabolism. *Sgpl1*$^{-/-}$ chimeras show an almost completely blunted hyperlipidemic response to western type diet (A-C) corresponding with a less pro-atherogenic plasma lipoprotein profile (D-F). VLDL and LDL particles of the *Sgpl1*$^{-/-}$ chimeras show decreased total cholesterol and phospholipid content, whereas HDL is enriched in total cholesterol and phospholipids. VLDL triglycerides content shows a similar decrease. This was likely attributable to impaired fat absorption, as seen by decreased serum cholesterol uptake (slope difference P<0.05) (G), rather than changes VLDL secretion, as this is even increased in *Sgpl1*$^{-/-}$ chimeras (slope difference P<0.05) (H), or lipoprotein processing by lipoprotein lipase (LPL) (I), which shows no differences. HL:hepatic lipase. *Sgpl1*$^{-/-}$ chimeras showed a minor decrease in liver weight (J) and hepatic total cholesterol content (TC) (K). Gene expression analysis of the liver indicated an induced activation status of macrophages, as the CD68 macrophage marker showed no difference (L), while MARCO expression, a cytokine regulated macrophage receptor, was increased by 7-fold (M). *P< 0.05, ***P< 0.001.

Remarkably, VLDL production appeared to be even increased in these animals as shown by the accelerated triglyceride accumulation in plasma after LPL-inhibition ($P<0.05$, Figure 9H). No changes were seen in LPL activity (Figure 9I). Overall these results point to altered intestinal lipid metabolism in *Sgpl1*$^{-/-}$ chimeras.

Liver morphology showed no remarkable changes, while at point of sacrifice both liver weight and hepatic total cholesterol content were moderately elevated (15%, $P<0.05$, Figure 9J, 9K). Hepatic triglyceride or phospholipid contents were unaffected. Next, we have examined hepatic expression of key genes in lipid metabolism. No significant changes were seen on genes involved in lipid homeostasis such as LRP-1 (low density lipoprotein receptor-related protein 1), Scd1 (stearoyl-coenzyme A desaturase 1), HMGCoA (hydroxymethylglutaryl-coenzyme A) reductase, SRBI (scavenger receptor class B, member 1), SREBP-1 (sterol regulatory element binding transcription factor), and MTP (microsomal triglyceride transfer protein) (data not shown), while only that of ABCA1 (ATP-binding cassette, sub-family A [ABC1], member 1) tended to be increased (+40%, $P=0.06$, data not shown). Evaluation of liver macrophage genes showed that, while the CD68 macrophage markers showed no difference (Figure 9L), MARCO (macrophage receptor with collagenous structure) expression, a cytokine regulated macrophage receptor, was increased by 7-fold ($P<0.001$, Figure 9M), reflecting macrophage activation in liver rather than cell influx.
Further assessment of intestine morphology did show prominent changes on villi and microvilli morphology, indicative for a decreased absorption capacity (Figure 10). Evaluation of the intestinal expression of key genes involved in lipid metabolism revealed increased levels of Niemann-Pick C1-like 1 (Npc1l1), which is an intestinal cholesterol transporter (1.5 fold, $P<0.05$, data not shown). Consistent with liver expression patterns, also intestinal MARCO expression was increased (5.5-fold; $P<0.001$, data not shown), while that of the CD68 macrophage marker showed no difference.

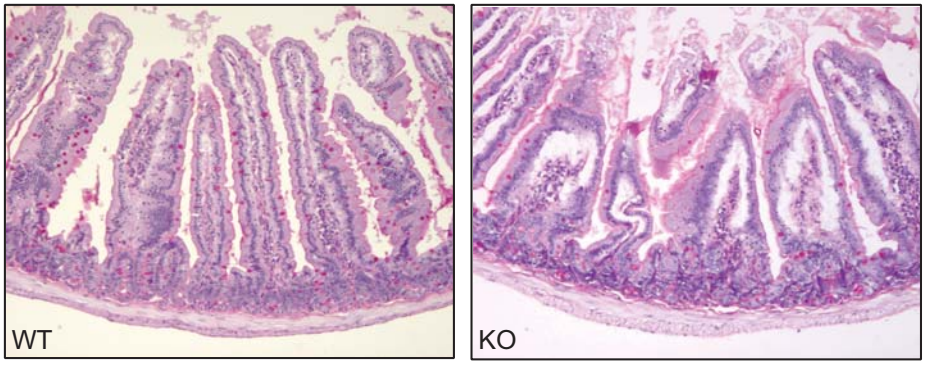


**Figure 10.** Effect of *Sgpl1*$^{-/-}$ chimerism on intestinal morphology. Example of the intestine of wild type (left) and *Sgpl1*$^{-/-}$ (right) transplanted animals. Duodenum of *Sgpl1*$^{-/-}$ transplanted animals shows atrophy of the duodenal mucosa characterized by shortened and blunted villi (PAS staining, 100x).

*Hematopoietic Sgpl1$^{-/-}$ chimeras show reduced atherosclerosis*

Morphometric quantification of Oil Red O-stained aortic root lesions of Western diet fed LDLr$^{-/-}$ chimeras revealed that plaque size of the *Sgpl1$^{-/-}$* transplanted mice was significantly decreased (35%, P=0.02) as compared to wild type transplanted mice ($1.05*10^5$ µm$^2$ versus $1.62*10^5$ µm$^2$, Figure 11A). Despite sharply increased circulating monocyte numbers, plaques from *Sgpl1$^{-/-}$* chimeras did not differ significantly with respect to MOMA-2-positive macrophages (Figure 11B). However, hematopoietic S1P lyase deficiency reduced CD3$^+$ T cell content in lesions and adventitial tissue, albeit not significantly (Figure 11C). While *Sgpl1$^{-/-}$* bone marrow transplantation attenuated lesion formation in the aortic root, it did not significantly affect the plaque collagen content (1.3 ± 1.0% versus 1.1 ± 0.3% in control animals).

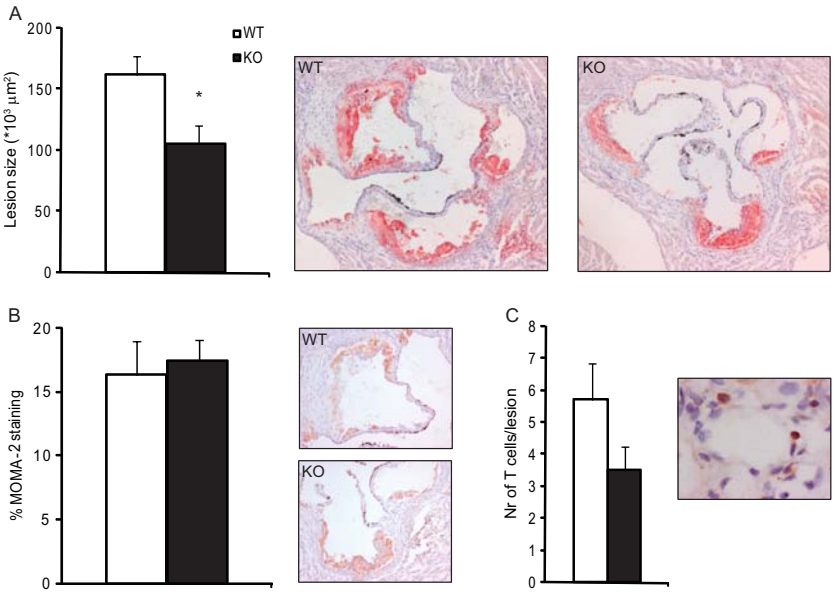


**Figure 11.** Effect of *Sgpl1$^{-/-}$* chimerism on aortic root lesions. (A) Lesion analysis of aortic root lesions shows that absence of hematopoietic S1P lyase decreases atherosclerotic lesion progression compared to control animals by 35%. (B) Although apparent monocytosis in the circulation was seen, morphological analysis showed no changes on macrophage content. (C) Conversely, a trend was observed towards a decreased T-cell content in the lesion (P=0.09). *P< 0.05.

## Discussion

S1P signaling is critical in the pathogenesis of several inflammatory diseases including ulcerating colitis, viral myocarditis, endotoxin-induced lung injury, or autoimmune encephalomyelitis[20-23]. Recent studies established the atheroprotective effect of exogenous S1P mimetics, such as FTY720, in mouse models of disease[19,25]. This sphingosine analogue can, in its phosphorylated form (FTY720-P), act on several S1P receptors. However, the relevance of endogenous S1P for the development of atherosclerosis has not been investigated to date. Here, we establish the critical importance of hematopoietic S1P lyase, a key enzyme responsible for intracellular

S1P degradation and maintenance of S1P gradients in the lymphoid system, for S1P dependent and independent lymphocyte trafficking. Moreover, we are the first to show that, similar to S1P mimetics, increased levels of endogenous S1P, as encountered in hematopoietic *Sgpl1* deficiency, ameliorates atherogenesis and leads to decreased T-cell influx into the lesion area, while leaving plaque macrophage content unaltered. This atheroprotective effect may be partly the result of the modulatory effects exerted by S1P on lymphocyte trafficking and other chemotactic signals and partly of the unexpected, quenched hyperlipidemic response to high fat diet leading to a less pro-atherogenic plasma lipoprotein profile. While *Sgpl1* deficiency also led to the expansion of the myeloid lineage and altered MCP-1 dependent monocyte trafficking, as well as inflammatory profile, these putatively pro-atherogenic effects of S1P were apparently insufficient to reverse the aforementioned atheroprotective effects on T lymphocytes and lipid profile.

Several mutually non-exclusive mechanisms may account for the diminished atherosclerosis development observed under conditions of enhanced endogenous S1P production. Obviously, the most dramatic effects of S1P lyase deficient bone marrow transplantation were noticed on lymphocyte counts and distribution. Lymphocytes are crucially involved in the propagation of inflammatory processes within the arterial wall and T-cell deficiency was repeatedly reported to attenuate atherogenesis. Decreased lymphocyte availability could therefore partly account for the reduced atherogenic response seen in S1P lyase deficient animals. The profound lymphopenia was a likely consequence of S1P gradient disruption, which are crucial for normal lymphocyte egress from lymphoid organs and therefore for proper immune effector function. This notion is supported by the altered surface expression pattern in the *Sgpl1*$^{-/-}$ chimeras of CCR7 and CXCR4, two $G_i\alpha$-coupled receptors transmitting retention signals for T cells in secondary lymphatic organs and regulating their distribution within T zones. Moreover, *in vivo* analysis of lymphocyte trafficking revealed severely perturbed homing of S1P lyase deficient splenocytes to spleen and lymph nodes as compared to wild type cells. Our observations, showing dramatically reduced number of lymphocytes in blood, lymph nodes and spleen, but only moderate changes in thymus T-cell populations, largely recapitulate the findings in $S1P_1$ deficient animals[10] and after systemic S1P lyase inhibition by THI[12]. In the latter study a functional desensitization of $S1P_1$ in lymphocytes exposed to severely increased S1P concentrations has been postulated. While $S1P_1$ expression levels were unchanged and $S1P_1^+$ T-cell subsets even enriched, $S1P_1$-mediated signaling per se has been not addressed and can thus not be excluded.

In addition to regulating lymphocyte trafficking, S1P was previously demonstrated to modulate several aspects of lymphocyte function. For instance, suppressed T-cell response to mitogenic stimuli, reduced migratory responses and decreased secretion of several T-cell specific cytokines including IL-2 were observed *in vitro* in lymphocytes exposed to S1P[19]. Previously, we demonstrated diminished splenocyte proliferation and cytokine production in LDLr$^{-/-}$ mice treated with an S1P mimetic, FTY720[19]. In the present study, we extend these findings to show impaired splenocyte proliferation in response to ConA in *Sgpl1*$^{-/-}$ splenocytes. In addition, the migratory response of both $CD4^+$ and $CD8^+$ T cells from blood to CCL19 was abolished in S1P lyase deficiency. Finally, the cytokine profiles of S1P lyase deficient animals suggested an attenuated T helper (Th)1 response, as evidenced by decreased IL-2

and IL-4 responses to CCL19 stimulation. A further indication of reduced lymphocyte activation in *Sgpl1*$^{-/-}$ chimeras was the almost complete absence of germinal centers in spleen. The quenched lymphocyte function in S1P lyase deficient mice was accompanied by a relative increase of $CD4^+CD25^+$ regulatory T (Treg) cells, known to suppress proliferation and IL-2 secretion by $CD4^+$ cytotoxic T-cells as well as to restrict Th cell-mediated antigen presentation. As suppressors of lymphocyte function, Treg cells are thought to exert potent anti-atherogenic effects. Actually, depletion or blockade of Treg cell function was repeatedly shown to aggravate atherosclerosis in mouse models of the disease[40]. Hence, the expansion of Treg cell population in hematopoietic S1P lyase deficiency may represent an additional mechanism, by which endogenous S1P inhibits development of atherosclerotic lesions in these mice.

While profound lymphopenia was the most striking feature of S1P lyase deficient mice, they were also characterized by moderately increased monocyte and neutrophil numbers in blood. This was likely a consequence of *de novo* overproduction in stromal tissue, a novel observation shown for the first time here. Despite persistent monocytosis, however, the plaque macrophage content remained unchanged in *Sgpl1* deficiency. Importantly, *Sgpl1*$^{-/-}$ chimeras displayed decreased MCP-1 levels in plasma and their bone marrow-derived macrophages showed considerably reduced ability to secrete MCP-1 both in the idle state and after stimulation with LPS. MCP-1 is a major chemokine not only driving stromal egress but also monocyte migration to inflammation sites such as atherosclerotic lesions in the vasculature[41,42]. A reduced MCP-1 production may thus underlie the unchanged macrophage content in atherosclerotic lesions of hematopoietic S1P lyase deficient animals despite the modest monocytosis in these mice. In this context, it is worth notice that reduced plasma MCP-1 levels and macrophage content in the lesion were also observed in ApoE$^{-/-}$ mice treated with FTY720[25]. In FTY720-treated LDLr$^{-/-}$ mice macrophages clearly showed a polarization towards a M2 phenotype as judged from the decreased pro-inflammatory IL-6 and nitrate and increased IL-1RA release, a marker for alternative macrophage activation[19]. However, *Sgpl1*$^{-/-}$ macrophages displayed a different, more pro-inflammatory phenotype with increased excretion and/or expression of IL-6, IL-12, TNF-α, and IL-1α, and lowered expression of IL-10, IL1-RA and arginase 1[24,43]. Overall, hematopoietic *Sgpl1* deficiency exerts rather contradictory effects favoring pro-inflammatory monocytosis and M1 polarization while at the same time reducing MCP-1-dependent monocyte influx into peripheral tissues.

Previous studies did not observe any beneficial effects on plasma lipid and lipoprotein alterations in mice treated with synthetic S1P mimetics[19,25,44]. In contrast, hematopoietic S1P lyase deficiency had profound effects on lipid homeostasis, directly linking S1P signaling to lipid and lipoprotein metabolism. The hyperlipidemic response to Western type diet feeding was severely blunted in *Sgpl1*$^{-/-}$ chimeras and these mice presented a considerably less atherogenic lipoprotein profile.This concurs with previous studies of Duivenvoorden *et al.* showing a dose-dependent inhibition of intestinal fat adsorption by S1P receptor-activating phytosphingolipids and concomitant reduction of plasma cholesterol and triglycerides in ApoE*3-Leiden mice[45]. Apparently S1P or analogues can directly or indirectly interfere with intermediary lipid metabolism. However, in the hematopoietic S1P lyase deficient animals the attenuated hyperlipidemic response to high cholesterol diet ascribed to disturbed intestinal fat absorption could be caused by aberrant intestinal microvilli architecture.

Interestingly, S1P homeostasis has been demonstrated to be pivotal in normal intestinal regeneration and function[46,47]. By contrast, no overt changes of hepatic lipid homeostasis were observed in *Sgpl1*$^{-/-}$ chimeras except that VLDL production appeared to be slightly increased, possibly as a compensatory measure counteracting the disproportional reduction in plasma lipids. In addition, plasma lipolysis rate was unaffected in these animals, which is in contrast to earlier findings on adipocytes treated with S1P[48].

In summary, hematopoietic S1P lyase is essential for maintenance of S1P gradients and its absence has profound effects not only on lymphoid surveillance but also on lymphocyte activity, stromal monocyte release and intestinal and hepatic lipid homeostasis. As a consequence, S1P lyase deficiency renders lymphocytes as well as monocytes refractory to chemotactic signaling pathways. Combined effects of hematopoietic S1P lyase deficiency translate into reduced atherosclerotic lesion formation, making S1P an interesting target for anti-atherosclerotic therapeutic approaches.

## Acknowledgments

The authors would like to thank S. van Heiningen and L. Seslia from the Leiden/Amsterdam Center for Drug Research for technical assistance.

## References


1. Spiegel, M., Milstien S. Sphingosine-1-phosphate: an enigmatic signaling lipid. *Nat Rev Mol Cell Biol.* 2003;4:397-407.
2. Gardell SE, Dubin AE, Chun J. Emerging medicinal roles for lysophospholipid signaling. *Trends Mol Med.* 2006;12:65-75.
3. Yatomi Y, Ohmori T, Rile G, Kazama F, Okamoto H, Sano T, Satoh K, Kume S, Tigyi G, Igarashi Y, Ozaki Y. Sphingosine 1-phosphate as a major bioactive lysophospholipid that is released from platelets and interacts with endothelial cells. *Blood.* 2000;96:3431-3438.
4. Hänel P, Andréani P, Gräler MH. Erythrocytes store and release sphingosine 1-phosphate in blood. *FASEB J.* 2007;21:1202-1209.
5. Mitra P, Oskeritzian CA, Payne SG, Beaven MA, Milstien S, Spiegel S. Role of ABCC1 in export of sphingosine-1-phosphate from mast cells. *Proc Natl Acad Sci U S A.* 2006;103:16394-16399.
6. Rosen H, Goetzl EJ. Sphingosine 1-phosphate and its receptors: an autocrine and paracrine network. *Nat Rev Immunol.* 2005;5:560-570.
7. Goetzl EJ, Rosen H. Regulation of immunity by lysosphingolipids and their G protein-coupled receptors. *J Clin Invest.* 2004;114:1531-1537.
8. Mandala S, Hajdu R, Bergstrom J, Quackenbush E, Xie J, Milligan J, Thornton R, Shei GJ, Card D, Keohane C, Rosenbach M, Hale J, Lynch CL, Rupprecht K, Parsons W, Rosen H. Alteration of lymphocyte trafficking by sphingosine-1-phosphate receptor agonists. *Science.* 2002;296:346-349.
9. Brinkmann V, Davis MD, Heise CE, Albert R, Cottens S, Hof R, Bruns C, Prieschl E, Baumruker T, Hiestand P, Foster CA, Zollinger M, Lynch KR. The immune modulator FTY720 Targets sphingosine 1-phosphate receptors. *J Biol Chem.* 2002;277:21453-21457.
10. Matloubian M, Lo CG, Cinamon G, Lesneski MJ, Xu Y, Brinkmann V, Allende ML, Proia RL, Cyster JG. Lymphocyte egress from thymus and peripheral lymphoid organs is dependent on S1P receptor 1. *Nature.* 2004;427:355-360.
11. Allende ML, Dreier JL, Mandala S, Proia RL. Expression of the sphingosine 1-phosphate receptor, S1P1, on T-cells controls thymic emigration. *J Biol Chem.* 2004;279:15396-15401.
12. Schwab SR, Pereira JP, Matloubian M, Xu Y, Huang Y, Cyster JG. Lymphocyte sequestration through S1P lyase inhibition and disruption of S1P gradients. *Science.* 2005;309:1735-1739.
13. Cyster JG. Chemokines, sphingosine-1-phosphate, and cell migration in secondary lymphoid organs. *Annu Rev Immunol.* 2005;23:127-159.
14. Taha TA, Hannun YA, Obeid LM. Sphingosine kinase: biochemical and cellular regulation and role in disease. *J Biochem Mol Biol.* 2006;39:113-131.
15. Venkataraman K, Thangada S, Michaud J, Oo ML, Ai Y, Lee YM, Wu M, Parikh NS, Khan F, Proia RL, Hla T. Extracellular export of sphingosine kinase-1a contributes to the vascular S1P gradient. *Biochem J.* 2006;397:461-471.
16. Garcia JG, Liu F, Verin AD, Birukova A, Dechert MA, Gerthoffer WT, Bamberg JR, English D. Sphingosine 1-phosphate promotes endothelial cell barrier integrity by Edg-dependent cytoskeletal rearrangement. *J Clin Invest.* 2001;108:689-701.
17. Bolick DT, Srinivasan S, Kim KW, Hatley ME, Clemens JJ, Whetzel A, Ferger N, Macdonald TL, Davis MD, Tsao PS, Lynch KR, Hedrick CC. Sphingosine-1-phosphate prevents tumor necrosis factor-alpha mediated monocyte adhesion to aortic endothelium in mice. *Arterioscler Thromb Vasc Biol.* 2005;25:976-981.
18. Gomez-Munoz A, Kong J, Salh B, Steinbrecher UP. Sphingosine-1-phosphate inhibits acid sphingomyelinase and blocks apoptosis in macrophages. *FEBS Lett.* 2003;539:56-60.
19. Nofer JR, Bot M, Brodde M, Taylor PJ, Salm P, Brinkmann V, van Berkel T, Assmann G, Biessen EA. FTY720, a synthetic sphingosine 1 phosphate analogue, inhibits development of atherosclerosis in low-density lipoprotein receptor-deficient mice. *Circulation.* 2007;115:501-508.
20. Miyamoto T, Matsumori A, Hwang MW, Nishio R, Ito H, Sasayama S. Therapeutic effects of FTY720, a new immunosuppressive agent, in a murine model of acute viral myocarditis. *J Am Coll Cardiol.* 2001;37:1713-1718.
21. Peng X, Hassoun PM, Sammani S, McVerry BJ, Burne MJ, Rabb H, Pearse D, Tuder RM, Garcia JG. Protective effects of sphingosine 1-phosphate in murine endotoxin-induced inflammatory lung injury. *Am J Respir Crit Care Med.* 2004;169:1245-1251.
22. Webb M, Tham CS, Lin FF, Lariosa-Willingham K, Yu N, Hale J, Mandala S, Chun J, Rao TS. Sphingosine 1-phosphate receptor agonists attenuate relapsing-remitting experimental autoimmune encephalitis in SJL mice. *J Neuroimmunol.* 2004;153:108-121
23. Fujii R, Kanai T, Nemoto Y, Makita S, Oshima S, Okamoto R, Tsuchiya K, Totsuka T, Watanabe M. FTY720 suppresses CD4+CD44highCD62L- effector memory T cell-mediated colitis. *Am J Physiol Gastrointest Liver Physiol.* 2006;291:G267-274.
24. Hansson GK, Libby P. The immune response in atherosclerosis: a double-edged sword. *Nat Rev*

*Immunol.* 2006;6:508-519.
25. Keul P, Tölle M, Lucke S, von Wnuck Lipinski K, Heusch G, Schuchardt M, van der Giet M, Levkau B. The sphingosine-1-phosphate analogue FTY720 reduces atherosclerosis in apolipoprotein E-deficient mice. *Arterioscler Thromb Vasc Biol.* 2007;27:607-613.
26. Van Veldhoven PP. Sphingosine 1-phosphate lyase deficient mice. *Chem Phys Lipids.* 2005;136:164-165.
27. Galvan C, Camoletto PG, Cristofani F, Van Veldhoven PP, Ledesma MD. Anomalous Surface Distribution of Glycosyl Phosphatidyl Inositol-anchored Proteins in Neurons Lacking Acid Sphingomyelinase. *Mol Biol Cell.* 2008;19:509-522.
28. Gijsbers S, Asselberghs S, Herdewijn P, Van Veldhoven PP. 1-O-Hexadecyl-2-desoxy-2-amino-sn-glycerol, a substrate for human sphingosine kinase. *Biochim Biophys Acta.* 2002;1580:1-8.
29. Varga G, Balkow S, Wild MK, Stadtbaeumer A, Krummen M, Rothoeft T, Higuchi T, Beissert S, Wethmar K, Scharffetter-Kochanek K, Vestweber D, Grabbe S. Active MAC-1 (CD11b/CD18) on DCs inhibits full T-cell activation. *Blood.* 2007;109:661-669.
30. Chomczynski P, Sacchi N. Single-step method of RNA isolation by acid guanidinium thiocyanate-phenol-chloroform extraction. *Anal Biochem.* 1987;162:156-159.
31. 't Hoen PA, Van der Lans CA, Van Eck M, Bijsterbosch MK, Van Berkel TJ, Twisk J. Aorta of ApoE-deficient mice responds to atherogenic stimuli by a prelesional increase and subsequent decrease in the expression of antioxidant enzymes. *Circ Res.* 2003;93:262-269.
32. Miller MJ, Wei SH, Parker I, Cahalan MD. Two-photon imaging of lymphocyte motility and antigen response in intact lymph node. *Science.* 2002;296:1869-1873.
33. Bot I, von der Thusen JH, Donners MM, Lucas A, Fekkes ML, de Jager SC, Kuiper J, Daemen MJ, van Berkel TJ, Heeneman S, Biessen EA. Serine protease inhibitor Serp-1 strongly impairs atherosclerotic lesion formation and induces a stable plaque phenotype in ApoE-/-mice. *Circ Res.* 2003;93:464-471.
34. Bligh EG, Dyer WJ. A rapid method of total lipid extraction and purification. *Can J Med Sci.* 1959;37:911-917.
35. Zechner R. Rapid and simple isolation procedure for lipoprotein lipase from human milk. *Biochim Biophys Acta.* 1990;1044:20–25.
36. Van Eck M, Zimmermann R, Groot PH, Zechner R, Van Berkel TJ. Role of macrophage-derived lipoprotein lipase in lipoprotein metabolism and atherosclerosis. *Arterioscler Thromb Vasc Biol.* 2000;20: E53-62.
37. Sancho D, Gómez M, Sánchez-Madrid F. CD69 is an immunoregulatory molecule induced following activation. *Trends Immunol.* 2005;26:136-140.
38. Shiow LR, Rosen DB, Brdicková N, Xu Y, An J, Lanier LL, Cyster JG, Matloubian M. CD69 acts downstream of interferon-alpha/beta to inhibit S1P1 and lymphocyte egress from lymphoid organs. *Nature.* 2006;440:540-544.
39. Hughes JE, Srinivasan S, Lynch KR, Proia RL, Ferdek P, Hedrick CC. Sphingosine-1-phosphate induces an antiinflammatory phenotype in macrophages. *Circ Res.* 2008;102:950-958.
40. Ait-Oufella H, Salomon BL, Potteaux S, Robertson AK, Gourdy P, Zoll J, Merval R, Esposito B, Cohen JL, Fisson S, Flavell RA, Hansson GK, Klatzmann D, Tedgui A, Mallat Z. Natural regulatory T cells control the development of atherosclerosis in mice. *Nat Med.* 2006;12:178-180.
41. Tsou CL, Peters W, Si Y, Slaymaker S, Aslanian AM, Weisberg SP, Mack M, Charo IF. Critical roles for CCR2 and MCP-3 in monocyte mobilization from bone marrow and recruitment to inflammatory sites. *J Clin Invest.* 2007;117:902-909.
42. Daly C, Rollins BJ. Monocyte chemoattractant protein-1 (CCL2) in inflammatory disease and adaptive immunity: therapeutic opportunities and controversies. *Microcirculation.* 2003;10:247-257.
43. Kamari Y, Werman-Venkert R, Shaish A, Werman A, Harari A, Gonen A, Voronov E, Grosskopf I, Sharabi Y, Grossman E, Iwakura Y, Dinarello CA, Apte RN, Harats D. Differential role and tissue specificity of interleukin-1alpha gene expression in atherogenesis and lipid metabolism. *Atherosclerosis.* 2007;195:31-38.
44. Klingenberg R, Nofer JR, Rudling M, Bea F, Blessing E, Preusch M, Grone HJ, Katus HA, Hansson GK, Dengler TJ. Sphingosine-1-phosphate analogue FTY720 causes lymphocyte redistribution and hypercholesterolemia in ApoE-deficient mice. *Arterioscler Thromb Vasc Biol.* 2007;27:2392-2399.
45. Duivenvoorden I, Voshol PJ, Rensen PC, van Duyvenvoorde W, Romijn JA, Emeis JJ, Havekes LM, Nieuwenhuizen WF. Dietary sphingolipids lower plasma cholesterol and triacylglycerol and prevent liver steatosis in APOE*3Leiden mice. *Am J Clin Nutr.* 2006;84:312-321.
46. Dragusin M, Wehner S, Kelly S, Wang E, Merrill AH Jr, Kalff JC, van Echten-Deckert G. Effects of sphingosine-1-phosphate and ceramide-1-phosphate on rat intestinal smooth muscle cells: implications for postoperative ileus. *FASEB J.* 2006;20:1930-1932.
47. Oskouian B, Saba J. Sphingosine-1-phosphate metabolism and intestinal tumorigenesis: lipid signaling strikes again. *Cell Cycle.* 2007;6:522-527.
48. Jun DJ, Lee JH, Choi BH, Koh TK, Ha DC, Jeong MW, Kim KT. Sphingosine-1-phosphate mod-

ulates both lipolysis and leptin production in differentiated rat white adipocytes. *Endocrinology.* 2006;147:5835-5844.